Random Close Packing in a Granular Model

by

David Aristoff   and   Charles Radin *

Mathematics Department, University of Texas, Austin, TX 78712

Abstract

We introduce a 2-dimensional lattice model of granular matter. We use a combination of proof and simulation to demonstrate an order/disorder phase transition in the model, to which we associate the granular phenomenon of random close packing.

September, 2009

PACS Classification: 45.70.Cc, 81.05.Rm, 05.70.Ce

0. Introduction.

Granular materials, such as a static pile of sand or salt grains sedimented in a fluid such as air, exhibit interesting characteristic behavior at certain volume fractions. For sand in air the lowest possible volume fraction (called the *random loose packing density*) is about 0.58, and the highest possible volume fraction is about 0.74. In other words a sand pile can exist with volume fraction anywhere in the interval (0.58, 0.74). Within this range there are also: the *critical state density*, about 0.60, and the *random close packing density*, about 0.64 [dG]. In this paper we consider a toy model for granular materials, the goal being to model granular behavior near the random close packing density. Our results support the interpretation in [Ra] of the phenomenon of random close packing as an *order/disorder phase transition*; we show in our model that at high density the system is sensitive to the boundary conditions while at low density it is not, with a perfectly sharp transition in between.

Our model is 2-dimensional and consists of nonoverlapping, parallel, hexagonal "grains" for which the centers (and corners) lie on sites of the planar triangular lattice: $\{m(1/2, \sqrt{3}/2) + n(1,0) \mid m, n \in \mathbb{Z}\}$ (see Figure 1).
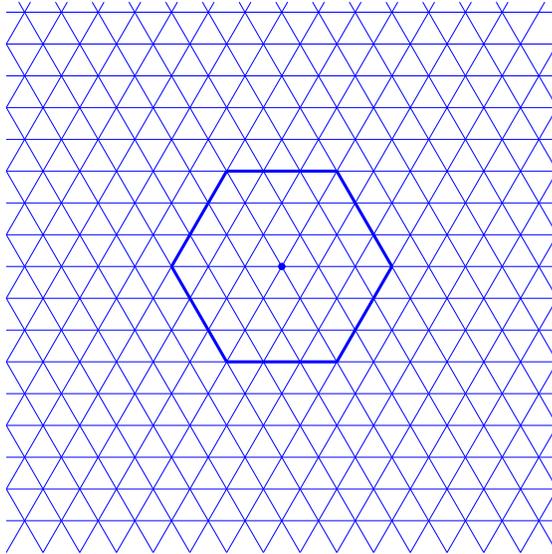

Figure 1. An hexagonal grain on the triangular lattice.

To account for the effects of gravity and friction we impose the condition that a configuration is allowed or *legal* only if each hexagonal grain intersects one of the three upper edges of another hexagonal grain, such that the latter grain has a center below that of the former (see Figure 2). Nearest neighbor sites in the lattice have separation 1, and the hexagons all have the same integral side length s. For the simulations

1

described below we use $s = 2, 3$ or 4; for our proofs any $s \geq 1$ suffices.

We use a "grand canonical" version of the Edwards model [EO] of granular matter; in this version the probability $Pr_V(A)$ of a legal configuration A of n particles in a fixed volume V is $e^{\mu n}/Z_V(\mu)$, where $\mu \in \mathbb{R}$ is a parameter and $Z_V(\mu)$ is the normalization constant (grand partition function); the "infinite volume limit" [Ru] is then taken, in which $V \to \mathbb{R}^2$.

Note that this model is a variation on the hard-core lattice-gas models of classical statistical mechanics, introduced by Lee and Yang in [LY], which use Peierls contours to prove a phase transition. (See [Gi, HP] for some later developments.) Specifically, in this method and for "extended" hard-cores in which particles are larger than a single lattice site, one proves that at all sufficiently high values of μ the model exhibits long range positional order, being sensitive at the middle of configurations to the precise relative location of the distant boundary, while at all sufficiently low values of μ the model is (easily) shown to behave as a dilute, disordered fluid, insensitive to the boundary.
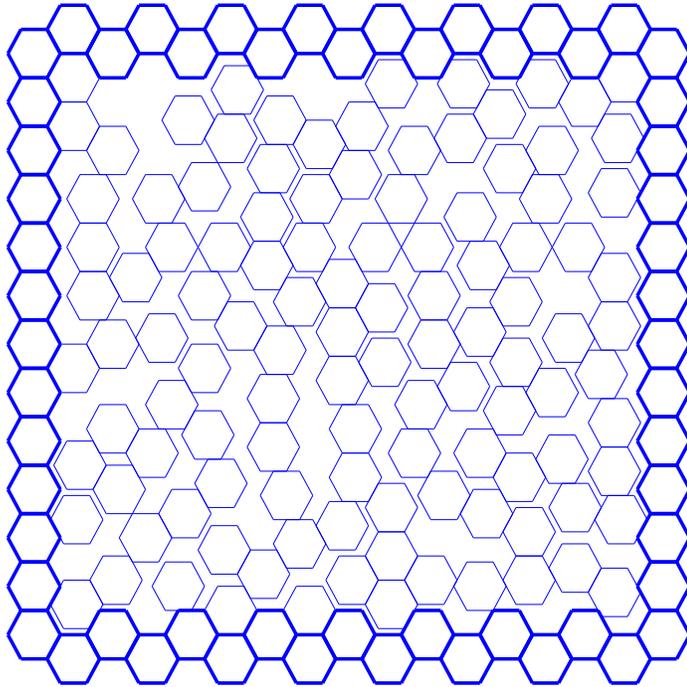

Figure 2. A legal configuration (boundary hexagons are in boldface).

For our granular model we are able to prove long range positional order for all

sufficiently high values of μ, but not disordered behavior at low μ. In place of a proof for the latter we have performed Monte Carlo simulations at low values of μ to demonstrate disorder. The proof for high μ is given in Section 1 and the numerical results for low μ are in Section 2.

We note that there was a previous granular adaption of the old hard hexagon models by Monasson and Pouliquen [MP]. Their model differs in several important details, for instance their use of periodic boundary conditions; more important is that they employ their model in a study of entropy rather than random close packing.

1. Proof for high μ.

Consider a regular triangular lattice with distance between nearest neighbor lattice sites equal to 1. We consider configurations of hard-core parallel regular *hexagons*, where a hexagon is centered at a lattice point and has side length equal to a fixed integer $s \geq 1$. The hexagons are all inside a square container V whose boundary consists of hexagons which intersect in full edges (see Figure 2).

We call a configuration of nonoverlapping hexagons inside the boundary *legal* if each hexagon h intersects one of the three upper edges of another hexagon h'. (We also require that h' is centered strictly below h.) We call h' a *support* of h. We let the number of hexagons inside the boundary (called *interior hexagons*), n, vary, and fix $\mu \geq 0$. The probability of seeing a given configuration A is $Pr(A) = e^{\mu n}/Z$, where n is the number of interior hexagons in A and $Z = Z(\mu)$ is the normalization. (For simplicity the notation will ignore dependence on the container V.)

Two hexagons h, h' are said to be *linked* if their intersection is a full edge (i.e. a line segment of length s), or if there is a sequence of hexagons $h_0 = h, h_1, ..., h_m = h'$ such that h_i intersects h_{i+1} in a full edge for $i = 0, ..., m-1$. In particular, the hexagons on the boundary are all linked. We are interested in the event that the origin lies inside a hexagon linked to a boundary hexagon; we call this event 0_{LB}.

A *triangle* is a closed regular triangle with side length 1 and vertices at lattice sites. Given a configuration A inside V, we define a *contour* in A to be one of the connected components of the union of all triangles in V not covered by hexagons in A, and all line segments in V of length strictly less than s which are intersections of neighboring hexagons in A. An *outer contour* is a contour which intersects a boundary hexagon or a hexagon linked to the boundary (see Figure 3). Note that the topological boundary of a contour C contains a closed curve γ which encloses an area containing the entire contour. We call the region enclosed by γ the *region enclosed by C*.

A *sublattice* is a set of points which are the centers of a collection of hexagons which tile the plane. There are $3s^2$ distinct sublattices. Note that any set of hexagons which are linked corresponds to a single sublattice; in particular the boundary hexagons define a sublattice which we call the *boundary sublattice*. We say that a hexagon is *on the boundary sublattice* if its center is in the sublattice defined by the boundary hexagons.

3

Definition 1. Consider a hexagon h of side length s centered at the origin. Let S be a set of $3s^2$ lattice sites in h such that S has exactly one representative of each sublattice. We are interested in the event that there is a hexagon centered in S which is on the boundary sublattice; we call this event O_B.
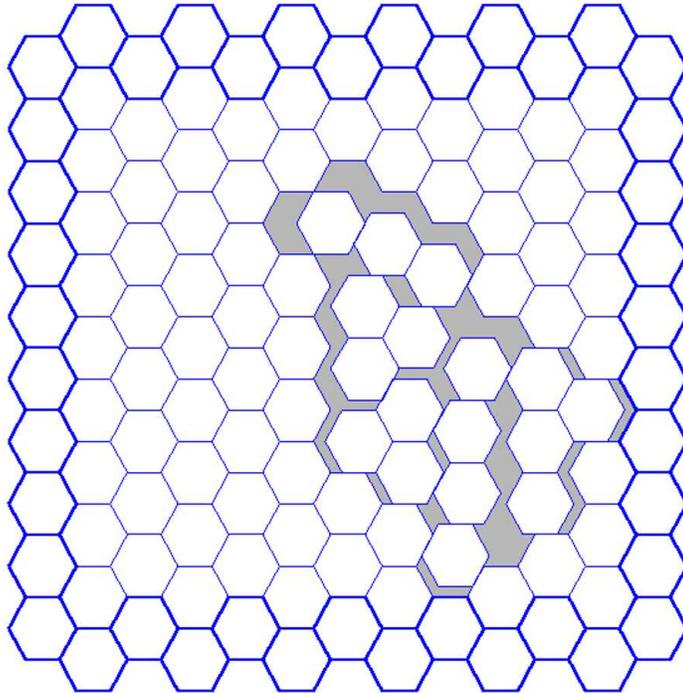

Figure 3. An outer contour (shaded region).

Lemma 1. If there is a hexagon centered in S which is not on the boundary sublattice, then this hexagon is not linked to the boundary.

Proof. If a hexagon centered in S is linked to the boundary, then it is on the sublattice defined by the boundary, since a set of linked hexagons corresponds to a single sublattice. ■

Lemma 2. If there is no hexagon centered in S, or if there is a hexagon centered in S not linked to the boundary, then there is an outer contour C such that the origin is in the region enclosed by C.

Proof. If there is no hexagon centered in S, then the origin itself is inside a contour and the result follows. Now assume there is a hexagon centered in S, and consider the contrapositive. If there is no outer contour enclosing the origin, then there is no contour at all enclosing the origin. Thus the hexagon centered in S is linked to the boundary. ■

4

Corollary 1. If there is no hexagon centered in S, or if there is a hexagon centered in S which is not on the boundary sublattice, then there is an outer contour enclosing the origin.

Proof. This follows from Lemmas 1 and 2. ∎

Let $[0_B]^c$ be the complement of the event 0_B. We will give an upper bound for $P([0_B]^c)$ by using a Peierls-type argument. We will first show that the probability of seeing a fixed contour is exponentially small for large μ. Then we will use a counting argument to get an upper bound on the number of possible contours.

The *size* of a contour is defined as its area in units of the area of a hexagon. We will see shortly that the size of a contour must be an integer. Given a contour C, let E be the region enclosed by C. The closures of the connected components of the complement of $C \cap E$ will be called *C-interior regions*. Note that the hexagons with edges on the topological boundary of a C-interior region R must be linked; we say such hexagons are on the *outside* of the R, and we say the remaining hexagons in R are on the *inside* of R.

We say that we *shift* a C-interior region R if we translate R while holding all other hexagons fixed. The translation must be given by a difference $x - y$ where x and y are lattice sites. Note that the relative positions of hexagons in a C-interior region R are unchanged by a shift.

Given a contour C, we say a C-interior region R is *on the boundary sublattice* if the hexagons on the outside of R are on the boundary sublattice.

Lemma 3. For any outer contour C there is a sequence of shifts of all of the C-interior regions such that in the resulting configuration, each of the shifted interior regions is on the boundary sublattice and no hexagons overlap one another.

Proof. For each site x on the boundary sublattice define a neighborhood N_x of x as follows. Let h be a regular hexagon of side length s centered at x. Then N_x consists of all lattice sites in h except those on any of the bottom three edges of h.

Note that the neighborhoods N_x are disjoint and together cover all the lattice sites. Create a sequence of shifts of the C-interior regions as follows. For each C-interior region R, take a hexagon h on the outside of R; assume h is centered at $y \in N_x$. Then shift R by $x - y$. Clearly, the hexagons on the outside of the shifted C-interior region are centered on the boundary sublattice. We must also check that the shifts do not create overlap.

To this end, let h_1 and h_2 be any two (distinct) hexagons in C-interior regions R_1 and R_2, and let h_1' and h_2' be the images of the hexagons under the shifts of R_1 and R_2 described in the preceding paragraph. If $R_1 = R_2$ then clearly h_1' and h_2' do not overlap. Thus assume $R_1 \neq R_2$, and suppose h_1 and h_2 are centered at y_1 and y_2, respectively. Then $y_1 \in N_{x_1}$ and $y_2 \in N_{x_2}$ for some $x_1 \neq x_2$, and h_1' and h_2' are centered at x_1 and x_2, respectively. Since x_1 and x_2 are both points on the boundary sublattice, h_1' and h_2' do not overlap, as desired. ∎

Note that the configuration produced by the protocol in Lemma 3 does not necessarily produce a *legal* configuration, just a configuration with no overlaps.

Lemma 4. The size of a contour C is an integer.

Proof. Consider a configuration produced by the protocol in Lemma 3. The new configuration has contours $C_1, C_2, \ldots, C_m$ in place of the original contour C. Since the protocol creates no overlaps, and since all the shifted C-interior regions remain within the region enclosed by C, the contours $C_1, C_2, \ldots, C_m$ have the same combined area as the contour C. Furthermore, the shifted C-interior regions are all on the boundary sublattice, so the hexagons bordering each C_i are all on the boundary sublattice. Thus we conclude that each C_i could be completely covered by nonoverlapping hexagons, all on the boundary sublattice. The result follows. ∎

Lemma 5. Fix an outer contour C of size k. There is a one-to-one correspondence between legal configurations A with exactly n interior hexagons and C as an outer contour, and legal configurations A' with exactly $n + k$ interior hexagons.

Proof. Let A_0 and A_1 be two distinct configurations with the outer contour C, and assume A_0 and A_1 have n_0 and n_1 interior hexagons, respectively. Using Lemmas 3 and 4, shift the C-interior regions of A_0 and A_1 to produce configurations $\tilde{A}_0$ and $\tilde{A}_1$ which both have contours $C_1, C_2, \ldots, C_m$ that can be completely covered by nonoverlapping hexagons. Cover these contours with nonoverlapping hexagons to produce configurations A'_0 and A'_1 having $n_0 + k$ and $n_1 + k$ interior hexagons, respectively. We claim first that A'_0 and A'_1 are legal configurations; of course it suffices to show that A'_0 is a legal configuration.

We have to show that each hexagon in A'_0 has a support. First consider a hexagon h in A'_0 in one of the shifted C-interior regions. Assume h is on the inside of the shifted region. Because shifts do not affect relative positions of hexagons inside the region, and since the configuration was legal before the shift, h must have a support. Now assume h is on the outside of the shifted region. If h does not have a support in the shifted region, then h must have had a support outside the region before shifting. Since the region $C_1 \cup \ldots \cup C_m$ is completely filled with hexagons, one of these must be a support of h. Finally consider a hexagon h not in one of the shifted C-interior regions. Since the contours $C_1, C_2, \ldots, C_m$ were completely filled with hexagons, clearly h has a support.

Next, we claim that A'_0 and A'_1 are distinct configurations. Note first that the C-interior regions of A_0 and A_1 have identical outsides, because the contour C defines these outsides. Thus there is an obvious pairwise association between the C-interior regions of A_0 and the C-interior regions of A_1. Since A_0 and A_1 are distinct, either at least one of these pairs of C-interior regions, say R_0 and R_1, must have different insides, or A_0 and A_1 must be different outside the region enclosed by C. In the latter case, the configurations A'_0 and A'_1 must be distinct, because the shifts done by the protocol in Lemma 3 do not change anything outside the region enclosed by C. In the former case, R_0 and R_1 have distinct insides. This of course does not change after

6

shifting, and so A_0' and A_1' are distinct. In either case A_0' and A_1' are distinct, so we have the desired correspondence. ∎

Lemma 6. Let C be a fixed contour of size k. The probability that a configuration has the contour C is at most $e^{-k\mu}$.

Proof. To prove this, we use the association in Lemma 5. Let Z be the normalization, and let E_C be the event that a configuration has the contour C. Let H_n be the number of legal configurations A having the contour C and n interior hexagons, and let H_n' be the number of legal configurations A' having $n+k$ interior hexagons. By Lemma 5 we have that $H_n' \geq H_n$, and of course we also have that $\sum_{n=0}^{\infty} e^{(n+k)\mu} H_n' \leq Z$. Thus, we have the estimate

$$Pr(E_C) = \frac{1}{Z} \sum_{n=0}^{\infty} e^{n\mu} H_n \leq \frac{\sum_{n=0}^{\infty} e^{n\mu} H_n}{\sum_{n=0}^{\infty} e^{(n+k)\mu} H_n'} \leq e^{-k\mu}$$

as desired. Note that this estimate is independent of the size of the container V. ∎

We are finished with half of the Peierls argument. Now we provide an upper bound on the number of contours of a given size. We do this by counting graphs whose vertices are triangles in a contour. Note that there are $6s^2$ triangles inside a hexagon.

Before we begin the counting argument we need the following well-known facts from graph theory:

Lemma 7 a. Let T be a spanning tree for a set of n points. Then T has $n-1$ edges.
　　　　　b. A graph G' produced by duplicating every edge of a graph G is Eulerian.

Now to count the contours, we make the following observation about the structure of a contour C. The union of all the triangles in a contour consists of several disjoint connected components. These components are joined to neighboring components by line segments in C of length strictly less than s; recall that such line segments are the intersections of neighboring hexagons. Thus, the minimum number of lattice segments in a path between triangles in neighboring components is at most $s - 1$, where by a *lattice segment* we mean a line segment joining nearest neighbor lattice sites. This leads to the following lemma.

Lemma 8. Suppose C is a contour of size k. Then $m = 6s^2k$ is the number of triangles in the contour. There is a sequence $(t_1, \ldots, t_{2m-1})$ of triangles in C such that each triangle in C is some t_i, and such that the mimimum number of lattice segments in a path joining t_i and t_{i+1} is $\leq s - 1$.

Proof. Let Z be a set of vertices, one for each triangle in C. Define the distance between vertices in Z as one plus the minimum number of lattice segments in a path joining the corresponding triangles in C. Partition Z into $Z_1, \ldots, Z_k$, where the Z_i

correspond to the connected components of the union of all the triangles in C. For each i, join two vertices in Z_i by an edge iff the distance between them is 1. Then one by one remove edges comprising cycles in each Z_i (this process is not necessarily unique).

Next, for each $i \neq j$, join $x \in Z_i$ to $y \in Z_j$ by an edge iff the distance between x and y is less than or equal to s. By preceding considerations we see that the resulting graph is connected. One by one remove edges comprising cycles to produce a tree T spanning all the vertices of Z. Note that all $(m-1)$ of the edges of T have length $\leq s$.

Now define a duplicate graph D which has the same vertices as T but which has two edges joining each pair of vertices which are joined by an edge in T. Then D is an Eulerian graph, so there is an Eulerian path, that is, a path Γ in D which traverses every edge exactly once. D has $2(m-1)$ edges, so Γ traverses $2(m-1)+1$ vertices, counting repeats. Clearly Γ traverses each vertex of T at least once. So take t_i to be the triangle corresponding to the ith vertex traversed by Γ. ∎

Lemma 9. The number of contours C of size k such that the origin is in the region enclosed by C is less than $p_m q^m$, where $m = 6s^2 k$, $p_m = 6m^2$ and $q = 36(s+1)^4$.

Proof. Using Lemma 8, for any contour C of size k we have a corresponding sequence $(t_1, \ldots t_{2m-1})$ of triangles in C, where $m = 6s^2 k$. Moreover, since the sequence covers all the triangles in C, distinct contours are associated with distinct sequences (note that a contour is totally defined by the positioning of its triangles). There are no more than $6m^2$ possible triangles that a contour enclosing the origin can contain, and given the position of the ith triangle there are at most $6(s+1)^2$ possibilities for the position of the $(i+1)$st. Since there are $2m - 1 < 2m$ total elements of the sequence, we may take $q = 36(s+1)^4$ and $p_m = 6m^2$ to get the desired result. ∎

Now we are ready to combine the two main ingredients of the Peierls argument into the final result:

Theorem 1. The probability that there is a hexagon centered in S which is on the boundary sublattice goes to 1 as μ goes to infinity. That is, $Pr(0_B) \to 1$ as $\mu \to \infty$.

Proof. By Corollary 1, Lemma 6 and Lemma 9, $Pr([0_B]^c)$ is bounded above by $\sum_{k=1}^{\infty} p_m (q^{6s^2} e^{-\mu})^k$, where again $m = 6s^2 k$. Since q^{6s^2} is a constant depending only on s, and since p_m is polynomial in k, we have that for μ sufficiently large, the summation bounding $Pr([0_B]^c)$ is arbitrarily small. Note that the estimate underlying this result is independent of the size of the container V. ∎

We have abbreviated this result by saying that at sufficiently large μ the system has long range order. We also have the following percolation result.

Corollary 2. The probability that the origin lies inside a hexagon linked to the boundary goes to 1 as μ goes to infinity; that is, $Pr(0_{LB}) \to 1$ as $\mu \to \infty$.

8

Proof. This follows by Lemma 2 and the same argument as in Theorem 1. ∎

2. Numerical Results for low μ.

We ran Markov chain Monte Carlo simulations on the model for a range of values of μ. We checked that the Monte Carlo runs were not sensitive to the initial condition (see Figure 4); since lower volume fraction initial conditions tended to equilibriate faster, we started the remaining Monte Carlo runs with void configurations.

If $\mu << 0$ typical configurations do not fill the container – see Figures 5 and 6 – and it is harder to develop useful data. Our goal in this section is to show that in the infinite volume limit the boundary has no influence near the origin for small μ. As the main object of our simulation we consider the quantity $p(\mu)$, defined as follows. First recall the set S defined in the preceding section, namely a set of representative lattice sites for each of the $3s^2$ different sublattices, such that S is contained inside a regular hexagon of side length s centered at the origin. Recall that we define a *sublattice* to be a set of lattice sites corresponding to the centers of a collection of hexagons which tile the plane.

Definition 2. For a fixed container V, we define $p(\mu)$ to be the probability that there is a hexagon h centered in S such that h is centered in the boundary sublattice.

Note that $p(\mu)$ is the same as the quantity $P(0_B)$, but here we emphasize its dependence on μ. We want to show that in the infinite volume limit, $p(\mu)$ is constant in some interval of positive length; its value there should be $1/3s^2$, where $3s^2$ is the number of sublattices. Recall from our results in the previous section that $p(\mu) \to 1$ as $\mu \to \infty$, *uniformly in system size.*

Our argument will concentrate on the interval $[1, 2]$ for μ. Simulation for μ inside this interval and inside the interval $[0, 10]$ suggests that in the infinite volume limit, $p(\mu)$ is indeed constant inside $[1, 2]$ (see Figures 7-12).

To obtain numerical estimates of $p(\mu)$ we considered the following functions on our Monte Carlo runs. For a configuration A we let $\delta(A) = 1$ if there is a hexagon in A centered at a point in S in the boundary sublattice; we let $\delta(A) = 0$ otherwise. We define $t(A) = 1$ if there is a hexagon in A centered at a point in S, and $t(A) = 0$ otherwise.

For systems ranging in volume from 276 to 1151 (in units of hexagon volume) we evaluated δ and t on configurations $A_1, A_2, \ldots$, and for each system size we consider the following statistic:

$$p_M := \frac{1}{T}[\delta(A_1) + \delta(A_2) + \cdots + \delta(A_M)]$$

where

$$T = t(A_1) + t(A_2) + \cdots + t(A_M)$$

So the expected value of p_M is exactly $p(\mu)$. We obtain confidence intervals for

9

p_M in the same way as in [AR]; in particular we determine the mixing time for our simulations using the biased autocorrelation function on volume fraction data, and then use the common method of batch means [Ge] with about 10 batches for each run, with batch size M chosen so that there are at least 5 mixing times per batch (except in the transition region).

If the boundary has no influence near the origin, hexagons should appear in each sublattice with equal probability, so we expect that the limiting value of $p(\mu)$ is exactly $1/(3s^2)$ for small μ. In Figures 7-12 we compare data from our Monte Carlo runs to the line $y = 1/(3s^2)$, with $s = 3$. For $\mu \in [0,4]$ the data suggests that $p(\mu)$ follows the line; then in the range $\mu \in [4,6]$, $p(\mu)$ increases to about 1; for $\mu > 6$, $p(\mu)$ stays near the line $y = 1$. In Figures 11-12 we consider more detailed data for μ in $[1,2]$. Our 95% confidence intervals cover the line $y = 1/(3s^2)$ more than 95% of the time, as appropriate.

We note that the transition region changes as s increases. In particular, as s increases the smallest value of μ such that $p(\mu) > 1/(3s^2)$ seems also to increase; compare Figures 9, 13, 14.

3. Conclusion.

Our argument is based on the behavior of $p(\mu)$ – the probability that a hexagon near the origin is on the same sublattice as the boundary hexagons – as a function of the parameter μ, the variable controlling average volume fraction. We have proven that for sufficiently large positive μ, $p(\mu)$ is greater than $1/(3s^2)$, and in fact $p(\mu)$ approaches 1 as $\mu \to \infty$, uniformly in the size of the system. In addition we have numerical evidence that in an interval above zero, $p(\mu)$ has the constant value $1/(3s^2)$ in the infinite volume limit, indicative of disorder. As the two types of behavior cannot be connected analytically we conclude [FR] that the model undergoes a phase transition at some positive μ. The transition can be seen in Figure 9, but it would take much more simulation to demonstrate singular behavior at a specific value of μ. Instead, our argument for the existence of a transition is based on failure of analyticity. (To use simulation to show that *dependence* on the boundary survives in the infinite volume limit requires careful study of the size of the simulation samples, while the burden is easier to show *independence* of the boundary, as we do.)

The transition we have found is of the order/disorder type since the long range order which we prove to hold at large μ is absent at low μ. We note that, as usual in hard-core lattice models [HP], our results only apply for a finite ratio s of hexagon size to lattice spacing; our upper bound on ordered behavior diverges as $s \to \infty$.
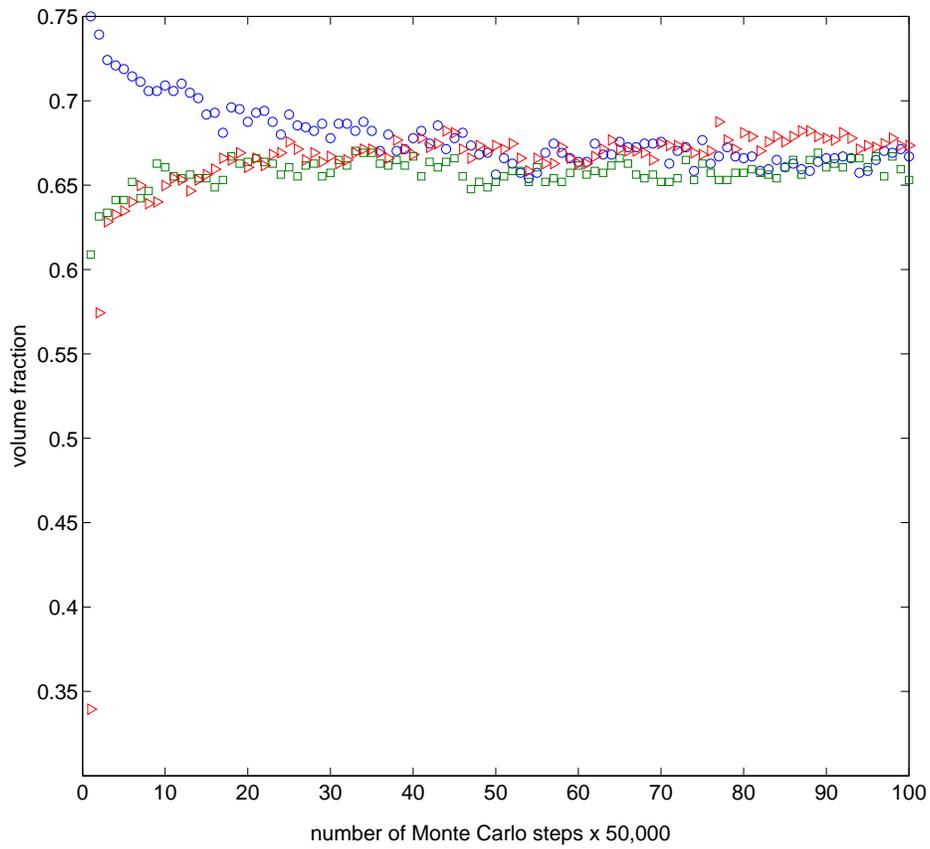
Figure 4. Plot of volume fraction versus number of moves, from three different initial volume fractions, for a system of volume 729 and $\mu = 1$.
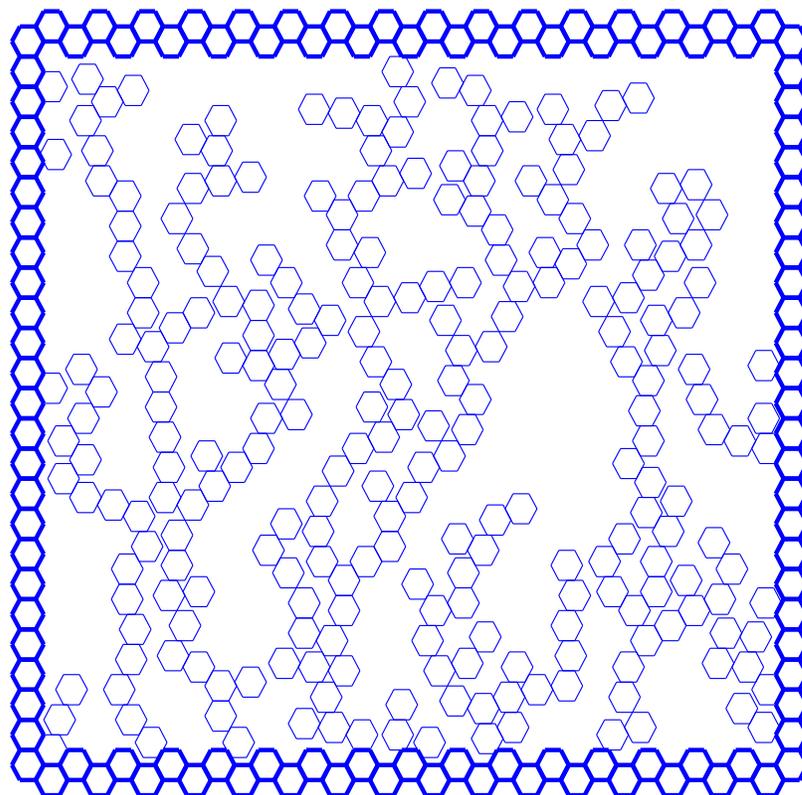
Figure 5. A configuration of 250 hexagons in equilibrium at $\mu = -4$, in a system of volume 729.
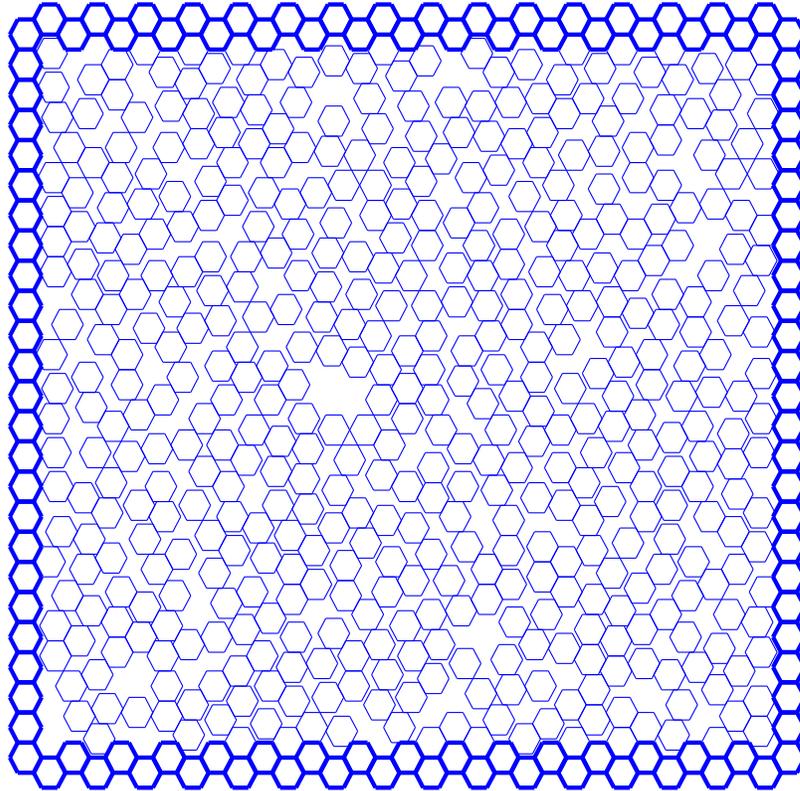
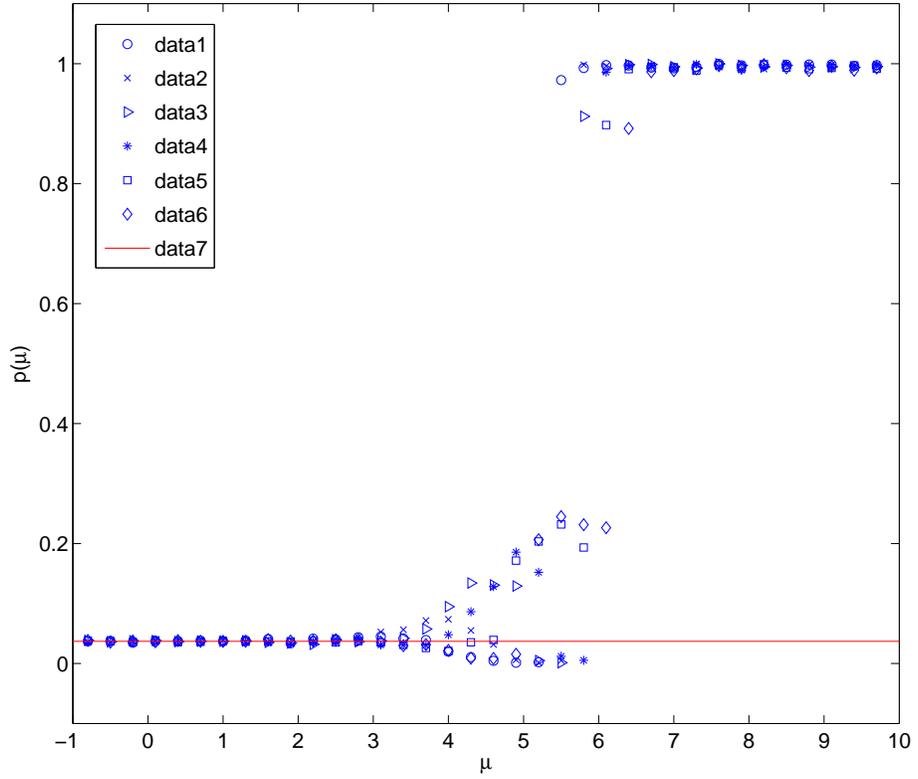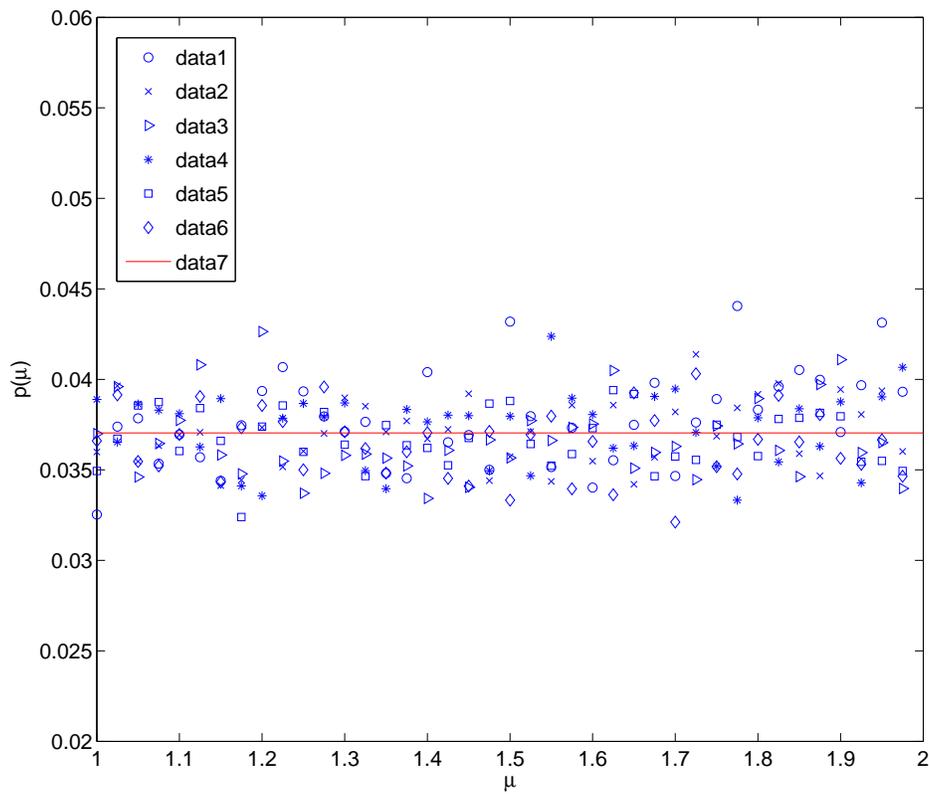Figure 6. A plot of a configuration in equilibrium at $\mu = 1$.

Figure 7. Plot of $p(\mu)$ vs. μ for systems of volume 276 (data1) to 1151 (data6), for $s = 3$. Data7 is the line $p(\mu) = \frac{1}{3s^2} = \frac{1}{27}$.
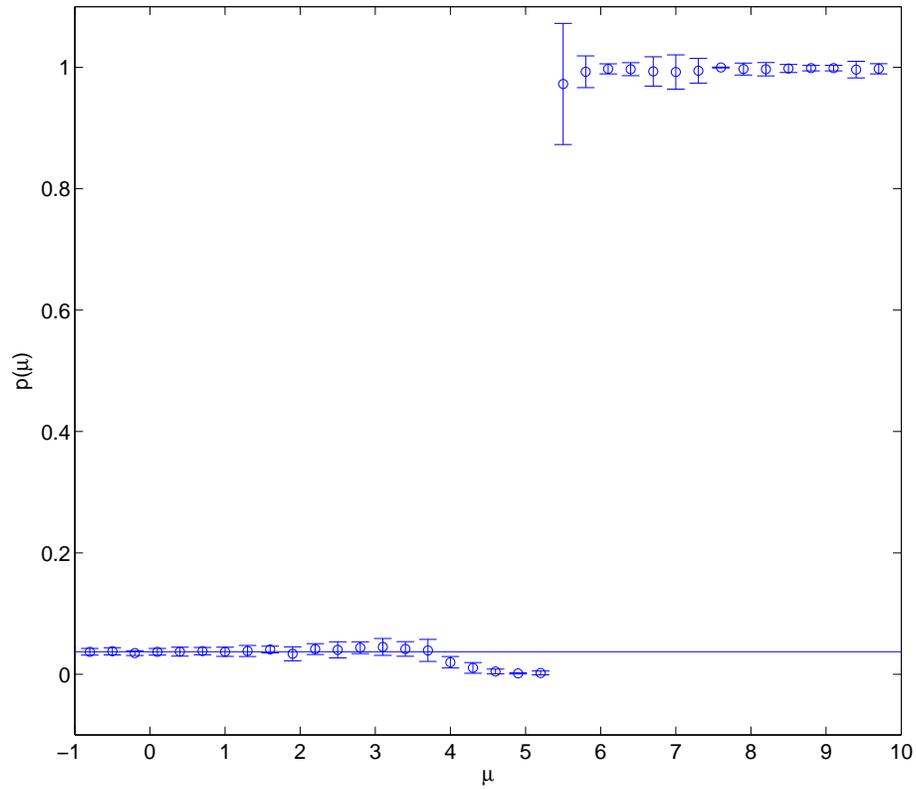
Figure 8. Plot of $p(\mu)$ vs. μ for systems of volume 276 (data1) to 1151 (data6), for $s = 3$. Data7 is the line $p(\mu) = \frac{1}{3s^2} = \frac{1}{27}$.

Figure 9. Plot of $p(\mu)$ vs. μ for a system of volume 276, with error bars, for $s = 3$. The line is $p(\mu) = \frac{1}{3s^2} = \frac{1}{27}$.

16
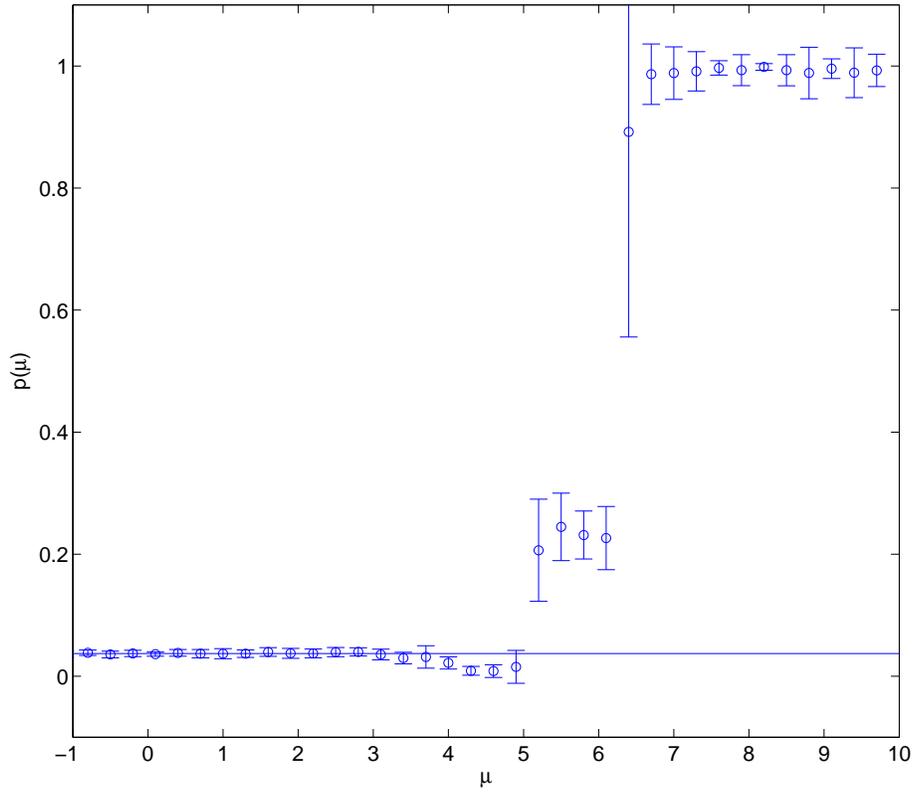
Figure 10. Plot of $p(\mu)$ vs. μ for a system of volume 1151, with error bars, for $s = 3$. The line is $p(\mu) = \frac{1}{3s^2} = \frac{1}{27}$.
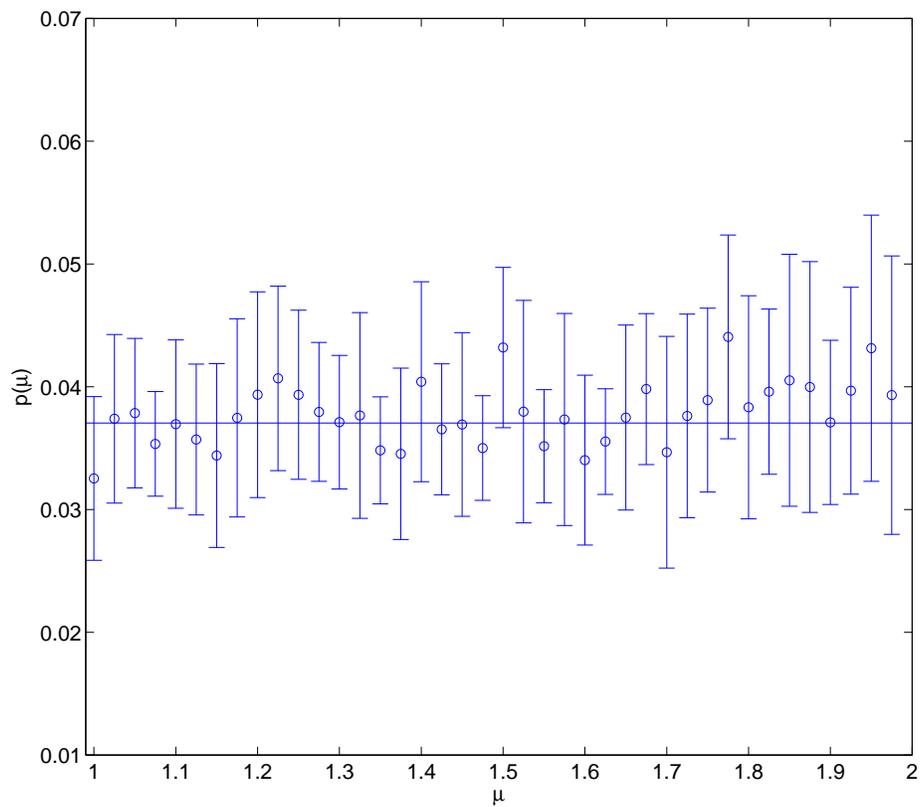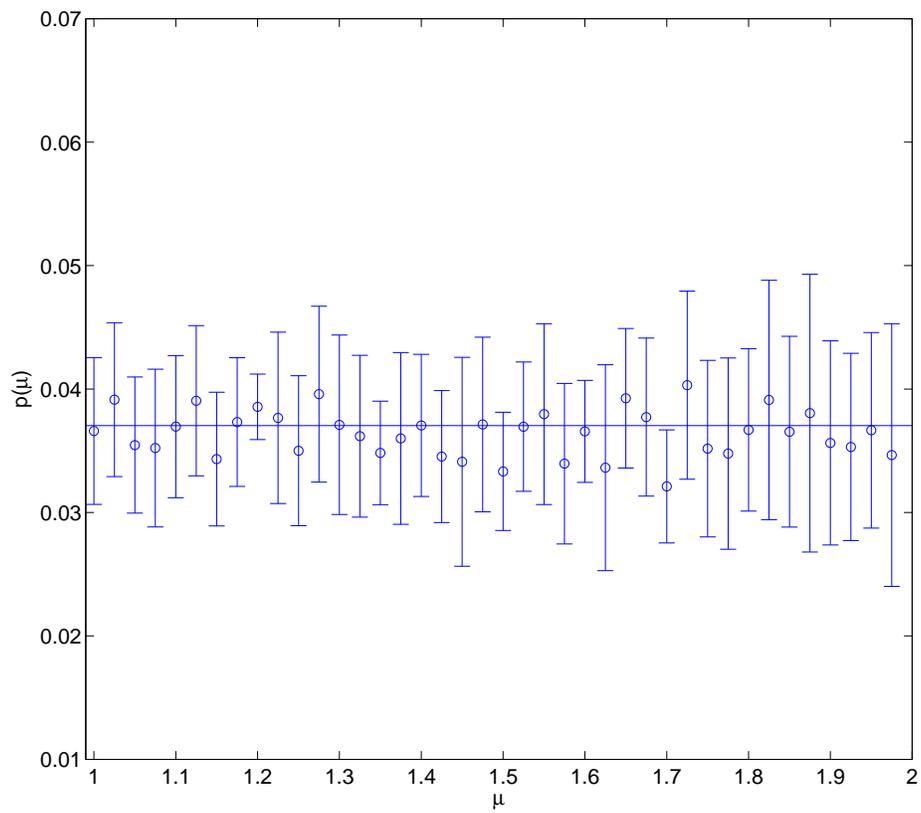
17

Figure 11. Plot of $p(\mu)$ vs. μ for a system of volume 276, with error bars, for $s = 3$. The line is $p(\mu) = \frac{1}{3s^2} = \frac{1}{27}$.

Figure 12. Plot of $p(\mu)$ vs. μ for a system of volume 1151, with error bars, for $s = 3$. The line is $p(\mu) = \frac{1}{3s^2} = \frac{1}{27}$.
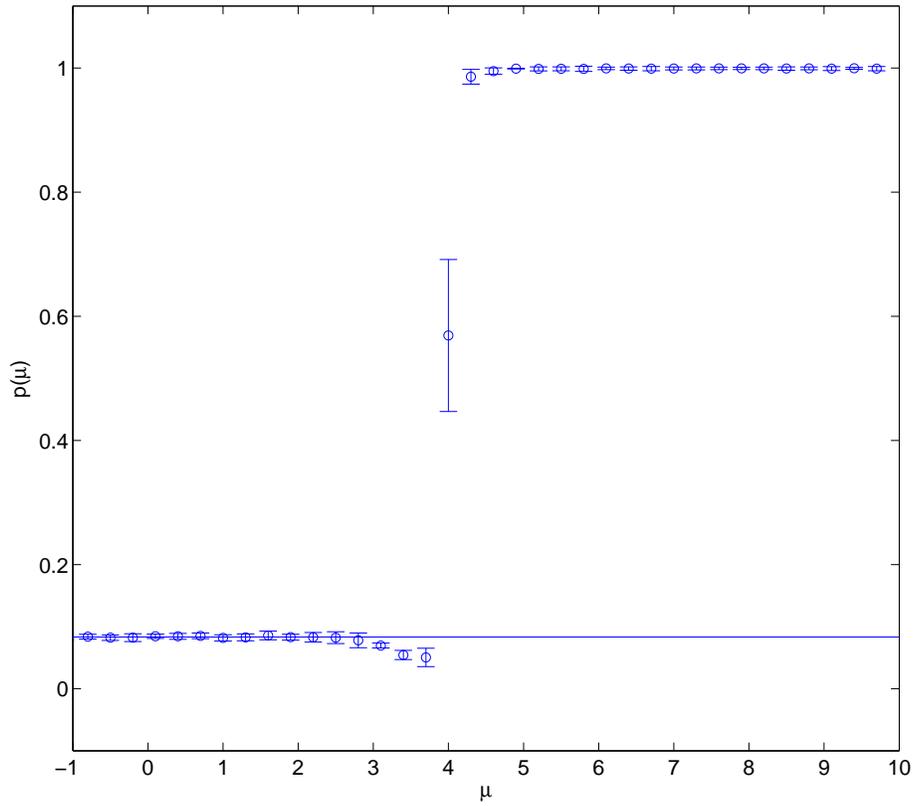
Figure 13. Plot of $p(\mu)$ vs. μ for a system of volume 276, for $s = 2$. The line is $p(\mu) = \frac{1}{3s^2} = \frac{1}{12}$.
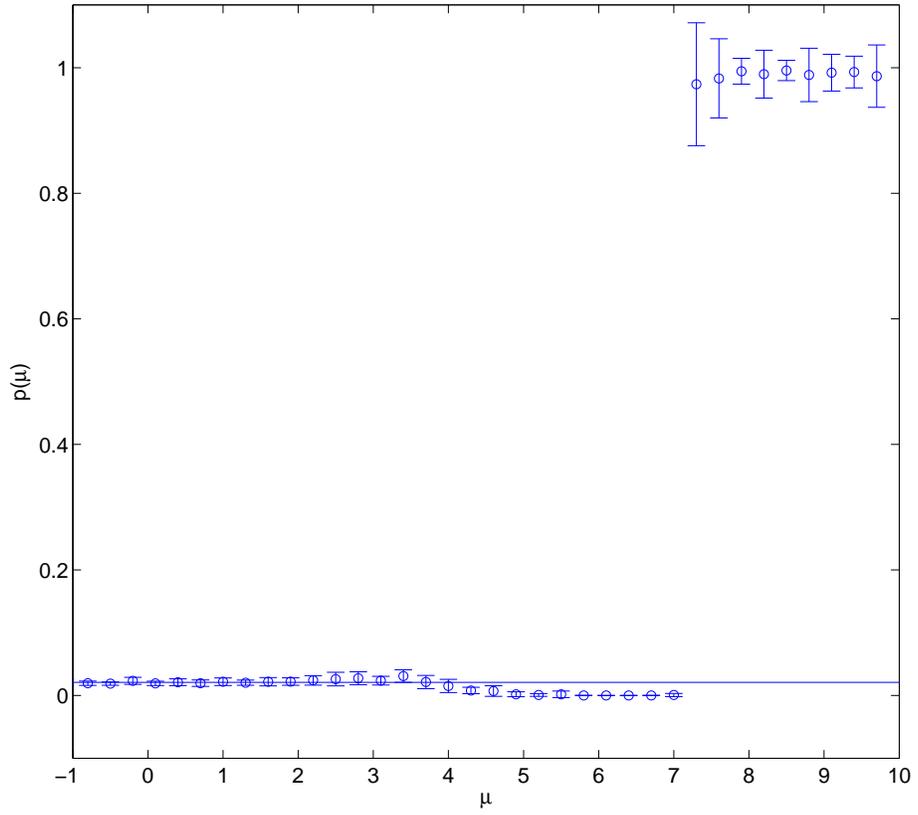
Figure 14. Plot of $p(\mu)$ vs. μ for a system of volume 276, for $s = 4$. The line is $p(\mu) = \frac{1}{3s^2} = \frac{1}{48}$.

21

References

[AR] D. Aristoff and C. Radin, Random loose packing in granular matter, J. Stat. Phys., 135(2009), 1-23.

[dG] P.G. de Gennes, Granular matter: a tentative view. Rev. Mod. Phys. 71 (1999) S374–S382.

[EO] S.F. Edwards and R.B.S. Oakeshott, Theory of powders, Physica A 157 (1989) 1080-1090.

[FR] M.E. Fisher and C. Radin, Definitions of thermodynamic phases and phase transitions, workshop report,
http://www.aimath.org/WWN/phasetransition/Defs16.pdf

[Ge] C.J. Geyer, Practical Markov chain Monte Carlo, Stat. Sci. 7 (1992) 473-483.

[Gi] J. Ginibre, On some recent work of Dobrushin, *Systèmes à un nombre infini de degrés de liberté*, CNRS, Paris, 1969, pp. 163-175.

[HP] O. J. Heilmann and E. Praestgaard, Phase transition of hard hexagons on a triangular lattice, J. Stat. Phys. 9 23-44 (1973).

[LY] T. D. Lee and C. N. Yang, Statistical Theory of Equations of State and Phase Transitions. II. Lattice Gas and Ising Model, Phys. Rev. 87 410-419 (1952).

[MP] R. Monasson and O. Pouliquen, Entropy of particle packings: an illustration on a toy model, Physica A 236 (1997) 395-410.

[Ra] C. Radin, Random close packing of granular matter, J. Stat. Phys. 131 (2008) 567-573.

[Ru] D. Ruelle, *Statistical Mechanics; Rigorous Results*, Benjamin, New York, 1969.